

Pharmacodynamic modeling of combined chemotherapeutic effects predicts synergistic activity of gemcitabine and trabectedin in pancreatic cancer cells

Xin Miao¹ · Gilbert Koch¹ · Robert M. Straubinger¹ · William J. Jusko¹

Received: 29 July 2015 / Accepted: 4 November 2015 / Published online: 25 November 2015
© Springer-Verlag Berlin Heidelberg 2015

Abstract

Purpose This study investigates the combined effects of gemcitabine and trabectedin (ecteinascidin 743) in two pancreatic cancer cell lines and proposes a pharmacodynamic (PD) model to quantify their pharmacological interactions.

Methods Effects of gemcitabine and trabectedin upon the pancreatic cancer cell lines MiaPaCa-2 and BxPC-3 were investigated using cell proliferation assays. Cells were exposed to a range of concentrations of the two drugs, alone and in combination. Viable cell numbers were obtained daily over 5 days. A model incorporating nonlinear cytotoxicity, transit compartments, and an interaction parameter ψ was used to quantify the effects of the individual drugs and combinations.

Results Simultaneous fitting of temporal cell growth profiles for all drug concentrations provided reasonable cytotoxicity parameter estimates (the cell killing rate constant K_{max} and the sensitivity constant KC_{50}) for each drug. The interaction parameter ψ was estimated as 0.806 for MiaPaCa-2 and 0.843 for BxPC-3 cells, suggesting that the two drugs exert modestly synergistic effects.

Conclusions The proposed PD model enables quantification of the temporal profiles of drug combinations over a range of concentrations with drug-specific parameters. Based upon these in vitro studies, trabectedin may have augmented benefit in combination with gemcitabine. The PD model may have general relevance for the study of other cytotoxic drug combinations.

Keywords Pharmacodynamic modeling · Drug interaction · Chemotherapeutic effect · Pancreatic cancer · Gemcitabine · Trabectedin

Introduction

Pancreatic adenocarcinoma is the fourth leading cause of cancer deaths in the USA, with a 5-year survival rate of only 6 % [1]. The current first-line therapy for patients with advanced pancreatic cancer is gemcitabine (GEMZAR, Eli Lilly, Indianapolis, IN) [2]. However, with a tumor response rate of <10 % [2], gemcitabine exhibits limited efficacy, so there exists a need for new treatment strategies and agents.

Drug combinations are used widely in cancer treatment because they offer the possibility of affecting cancer cells through different molecular mechanisms. Gemcitabine is often used with a DNA-damaging agent [3]. Trabectedin (YONDELIS[®], Et 743; PharmaMar S.A.U., Madrid, Spain) is a potent DNA-interacting compound that was isolated from the marine organism *Ecteinascidia turbinata* [4] and is now produced synthetically [5]. It was approved by the European Medicines Agency for the treatment of soft tissue sarcoma and platinum-sensitive relapsed ovarian cancer and was approved by the FDA on Oct. 23, 2015, for treatment of patients with advanced soft tissue sarcomas. Both gemcitabine and trabectedin target DNA. Gemcitabine is a nucleoside analog that requires intracellular phosphorylation after entering cells through a nucleoside transporter [6]. Gemcitabine triphosphate (dFdCTP) is incorporated into DNA and RNA and causes stalling of DNA replication. Trabectedin has a unique mechanism of action; it is composed of tetrahydroisoquinoline rings (A and B) that can form a covalent bond in the DNA minor groove at the

✉ William J. Jusko
wjusko@buffalo.edu

¹ Department of Pharmaceutical Sciences, School of Pharmacy and Pharmaceutical Sciences, State University of New York at Buffalo, Buffalo, NY 14214, USA

N2 position of guanine. The tetrahydroisoquinoline (subunit C) also interacts with DNA-binding proteins [7]. Both gemcitabine and trabectedin are cell cycle-specific agents [8–11]. Trabectedin can also inhibit the expression of oncogenes involved in drug resistance and genes involved in DNA repair pathways [12]. In combination, trabectedin may work synergistically with gemcitabine by blocking cell cycle progression and inducing apoptosis.

In a phase I pharmacokinetic study in patients with advanced solid tumors, gemcitabine followed by trabectedin showed no pharmacokinetic interaction [13]. However, pharmacodynamic studies of drug interactions between gemcitabine and trabectedin have not been reported. Therefore we examined the chemotherapeutic effects of gemcitabine and trabectedin in two pancreatic cancer cell lines.

Traditional methods [14, 15] to model drug–drug interactions such as the response-surface approach characterize data from a large range of concentrations at one time point. However, the dimension of time is not considered. Furthermore fitted parameters may vary with drug exposure time, concentration, and schedule [16]. More advanced approaches can include cell or tumor dynamics in order to characterize time-dependent data [16–18]. Here we advance PD modeling of drug interactions by extending the single-drug chemotherapy model of Lobo et al. [19] to characterize simultaneously both single- and combined drug effects, and add an interaction parameter ψ [20, 21] to quantify cytotoxic effects of the combinations. This approach can be applied in general to characterize drug combination effects in dimensions of both time and concentration.

Materials and methods

Experimental methods

Drugs and reagents

Gemcitabine hydrochloride from Eli Lilly (Indianapolis, IN) was prepared as a 50 mM stock solution in sterile double-distilled water and stored as aliquots at -20°C . Trabectedin, obtained as a gift from PharmaMar (Madrid, Spain), was prepared by dissolution in dimethylsulfoxide (DMSO) at a concentration of 1 mM, and stored at -20°C . Fresh dilutions were prepared for each experiment. The highest concentration of trabectedin added to cells resulted in a final concentration of $<0.1\%$ (v/v) DMSO in the culture medium.

Cell culture

In vitro experiments were performed with two human pancreatic cancer cell lines, MiaPaCa-2 and BxPC-3, which

were obtained from American Type Culture Collection (Manassas, VA). Media and serum were obtained from Cellgro (Manassas, VA). MiaPaCa-2 cells were cultured in DMEM supplemented with 10 % (v/v) fetal bovine serum (Atlanta Biological, Lawrenceville, VA), and BxPC-3 cells were cultured in RPMI 1640 with 10 % (v/v) fetal bovine serum and 1 % (v/v) sodium pyruvate (Gibco BRL, Gaithersburg, MD). Both cell lines were grown in monolayer culture at 37°C in a humidified atmosphere with 5 % CO_2 in 75-cm^2 tissue culture flasks (BD Biosciences, Bedford, MA).

Cell proliferation assay

Aliquots of approximately 2.0×10^4 cells were seeded in 24-well culture plates (BD Biosciences, Bedford, MA) with 1 mL fresh medium and allowed to adhere overnight. Then cells were exposed to increasing concentrations of gemcitabine and trabectedin alone and combined (Table 1). Triplicate wells were used for each exposure time and drug concentration. Control treatments consisted of sterile double-distilled water or DMSO as appropriate. Sixteen different combinations of drug concentrations spanning a reasonable range were selected. Cell counts were obtained every day for 5 days. Cell monolayers were washed twice with PBS (Gibco, Grand Island, NY), detached with trypsin, and counted using a Coulter Counter (Beckman Coulter, Hialeah, FL).

Mathematical modeling

Determination of IC_{50}

To select reasonable pairs of drug concentrations for the dynamic study, the IC_{50} of both drugs as single agents was determined over an exposure time of 3 days. Concentration–response curves were fitted with the inhibitory sigmoidal Hill function:

$$R = R_0 \left(1 - \frac{I_{\max,d} C_d^{\gamma_d}}{IC_{50,d}^{\gamma_d} + C_d^{\gamma_d}} \right) \quad (1)$$

where R is the cell number, R_0 is the cell number in the absence of drug, $I_{\max,d}$ is the maximum growth inhibition, $IC_{50,d}$ is the concentration that causes 50 % of the maximum effect, γ_d is the Hill coefficient, and C_d is the concentration of the corresponding drug, where d signifies either gemcitabine or trabectedin.

Pharmacodynamic modeling

Cell growth in the control group was described by the logistic growth function [22]:

Table 1 Concentrations of gemcitabine (G) and trabectedin (T) tested as single agents and combinations

Cell line	Drug	Cell proliferation assay Concentration (nM)
MiaPaCa-2	Gemcitabine (G)	0, 10, 15, 23, 30, 45, 100, 1000
	Trabectedin (T)	0, 0.6, 0.8, 1, 1.5, 3, 10, 100
	Combinations	0G + 0T, 15G + 0.6T, 15G + 0.8T, 15G + 1T, 15G + 1.5T
		23G + 0.6T, 23G + 0.8T, 23G + 1T, 23G + 1.5T
BxPC-3	Gemcitabine (G)	0, 11, 17, 23, 34, 68, 100, 1000
	Trabectedin (T)	0, 0.5, 0.7, 0.9, 1.1, 3, 10, 100
	Combinations	0G + 0T, 11G + 0.5T, 11G + 0.7T, 11G + 0.9T, 11G + 1.1T
		17G + 0.5T, 17G + 0.7T, 17G + 0.9T, 17G + 1.1T
		23G + 0.5T, 23G + 0.7T, 23G + 0.9T, 23G + 1.1T
		34G + 0.5T, 34G + 0.7T, 34G + 0.9T

$$\frac{dR}{dt} = k_g R \left(1 - \frac{R}{R_{ss}} \right) \quad R(0) = R_0 \quad (2)$$

where R is the cell number at time t , k_g is the first-order growth rate constant, R_{ss} is the cell number at steady state, and R_0 is the cell number at time zero.

Drug concentrations were assumed to be constant during the period of the experiment. Transit compartments were included in the model in order to capture the delay between drug exposure and the nonlinear cytotoxic effects, as proposed by Lobo et al. [19]. The temporal delay could arise from multiple intracellular steps, such as gemcitabine phosphorylation, DNA incorporation, cellular signal transduction cascades, and the time necessary for cytotoxic effects of the drugs to become established. The differential equations for gemcitabine or trabectedin (denoted by d , where Gem stands for gemcitabine and Et743 stands for trabectedin) are:

$$K_d = \frac{K_{max,d} C_d^{\gamma_d}}{K C_{50,d}^{\gamma_d} + C_d^{\gamma_d}} \quad (3a)$$

$$\frac{dK_{1,d}}{dt} = \frac{1}{\tau_d} (K_d - K_{1,d}) \quad K_{1,d}(0) = 0 \quad (3b)$$

$$\frac{dK_{2,d}}{dt} = \frac{1}{\tau_d} (K_{1,d} - K_{2,d}) \quad K_{2,d}(0) = 0 \quad (3c)$$

$$\frac{dK_{3,d}}{dt} = \frac{1}{\tau_d} (K_{2,d} - K_{3,d}) \quad K_{3,d}(0) = 0 \quad (3d)$$

$$\frac{dK_{4,d}}{dt} = \frac{1}{\tau_d} (K_{3,d} - K_{4,d}) \quad K_{4,d}(0) = 0 \quad (3e)$$

$$\frac{dR}{dt} = k_g R \left(1 - \frac{R}{R_{ss}} \right) - K_{4,d} R \quad R(0) = R_0 \quad (3f)$$

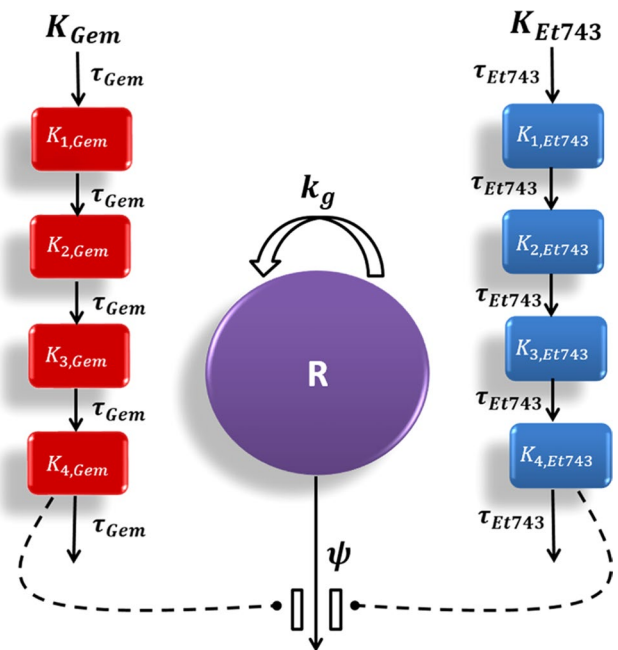


Fig. 1 Schematic of the PD model for combination effects of gemcitabine (Gem) and trabectedin (Et743) on pancreatic cancer cells. Definitions of parameters for the model and Eq. (4) are listed in Table 3. Solid lines with arrows indicate turnover of the indicated response. Dashed lines ending in closed circles indicate that an effect is being exerted by the connected factors

where $K_{max,d}$ is the maximum killing rate of the single agent, $K C_{50,d}$ is the sensitivity constant, γ_d is the Hill coefficient, C_d is the concentration of drug d (gemcitabine or trabectedin), K_d represents the cytotoxicity function, and $K_{i,d}$ are transit steps. The transit time between compartments is τ_d .

For the drug combinations, the PD model as shown in Fig. 1 operates as follows:

$$K_{Gem} = \frac{K_{max,Gem} C_{Gem}^{\gamma_{Gem}}}{(\psi KC_{50,Gem})^{\gamma_{Gem}} + C_{Gem}^{\gamma_{Gem}}} \tag{4a}$$

$$\frac{dK_{1,Gem}}{dt} = \frac{1}{\tau_{Gem}} (K_{Gem} - K_{1,Gem}) \quad K_{1,Gem}(0) = 0 \tag{4b}$$

$$\frac{dK_{i,Gem}}{dt} = \frac{1}{\tau_{Gem}} (K_{i-1,Gem} - K_{i,Gem})$$

$$K_{i,Gem}(0) = 0 \quad i = 2, \dots, 4 \tag{4c}$$

$$K_{Et743} = \frac{K_{max,Et743} C_{Et743}^{\gamma_{Et743}}}{KC_{50,Et743}^{\gamma_{Et743}} + C_{Et743}^{\gamma_{Et743}}} \tag{4d}$$

$$\frac{dK_{1,Et743}}{dt} = \frac{1}{\tau_{Et743}} (K_{Et743} - K_{1,Et743}) \quad K_{1,Et743}(0) = 0 \tag{4e}$$

$$\frac{dK_{j,Et743}}{dt} = \frac{1}{\tau_{Et743}} (K_{j-1,Et743} - K_{j,Et743})$$

$$K_{j,Et743}(0) = 0 \quad j = 2, \dots, 4 \tag{4f}$$

$$\frac{dR}{dt} = k_g R \left(1 - \frac{R}{R_{ss}} \right) - (K_{4,Gem} + K_{4,Et743}) R \quad R(0) = R_0 \tag{4g}$$

where ψ is the drug interaction parameter. If ψ equals 1, effects of the combination are additive, whereas ψ smaller than 1 signifies synergism and ψ greater than 1 indicates antagonism. In this study, additivity was defined as the summation of killing effects of gemcitabine ($K_{4,Gem}$) and trabectedin ($K_{4,Et743}$). Statistical significance is judged by the confidence limit of the ψ value not exceeding 1.

Derivation of threshold concentration

The concept of a threshold concentration $C_{T,d}$ was employed to describe the drug concentration required to cause either cell growth inhibition or cytotoxic effects. Necessary calculations are presented in the “Appendix.”

For single-drug effects, the threshold concentration is described as:

$$C_{T,d} = \left(\frac{k_g KC_{50,d}^{\gamma_d} R_{ss} - k_g R_0 KC_{50,d}^{\gamma_d}}{K_{max,d} R_{ss} - k_g R_{ss} + k_g R_0} \right)^{\frac{1}{\gamma_d}} \tag{5}$$

If $C_d < C_{T,d}$, the drug exhibits concentration-dependent inhibition of cell net growth, and cell number will increase and eventually approach a new plateau R'_{ss} that is greater than R_0 . In contrast, if $C_d > C_{T,d}$, the drug

exhibits cytotoxic effects and the dead cell population finally exceeds the dividing population; cell numbers approach a new steady state R'_{ss} that is smaller than R_0 . In both cases, R'_{ss} can be calculated by the equation:

$$R'_{ss} = \max \left\{ 0, \frac{R_{ss}}{k_g} \left(k_g - \frac{K_{max,d} C_d^{\gamma_d}}{KC_{50,d}^{\gamma_d} + C_d^{\gamma_d}} \right) \right\} \tag{6}$$

The drug concentration required for complete cell eradication is:

$$C_{E,d} = \left(\frac{k_g KC_{50,d}^{\gamma_d}}{K_{max,d} - k_g} \right)^{\frac{1}{\gamma_d}} \tag{7}$$

A similar concept has been utilized previously to estimate the drug concentration required for tumor eradication [23], and it was reported that $C_{E,d}$ and human clearance CL_h correlate highly with clinically relevant doses [24].

For drug combination effects, the steady state is given by:

$$R'_{ss} = \max \left\{ 0, \frac{R_{ss}}{k_g} \left(k_g - \frac{K_{max,Gem} C_{Gem}^{\gamma_{Gem}}}{(\psi KC_{50,Gem})^{\gamma_{Gem}} + C_{Gem}^{\gamma_{Gem}}} - \frac{K_{max,Et743} C_{Et743}^{\gamma_{Et743}}}{KC_{50,Et743}^{\gamma_{Et743}} + C_{Et743}^{\gamma_{Et743}}} \right) \right\} \tag{8}$$

Similarly, if $R'_{ss} > R_0$, the combination exhibits cell net growth inhibition, and if $R'_{ss} < R_0$, the combination exerts cytotoxic effects. If the concentrations used for the combination fulfill the condition:

$$\frac{K_{max,Gem} C_{Gem}^{\gamma_{Gem}}}{(\psi KC_{50,Gem})^{\gamma_{Gem}} + C_{Gem}^{\gamma_{Gem}}} + \frac{K_{max,Et743} C_{Et743}^{\gamma_{Et743}}}{KC_{50,Et743}^{\gamma_{Et743}} + C_{Et743}^{\gamma_{Et743}}} = k_g \tag{9}$$

then the drugs cause cell eradication. Solving Eq. (9) with respect to C_{Et743} yields:

$$C_{Et743} = \left(\frac{KC_{50,Et743}^{\gamma_{Et743}} P}{K_{max,Et743} - P} \right)^{\frac{1}{\gamma_{Et743}}} \tag{10a}$$

where

$$P = k_g - \frac{k_g R'_{ss}}{R_{ss}} - \frac{K_{max,Gem} C_{Gem}^{\gamma_{Gem}}}{(\psi KC_{50,Gem})^{\gamma_{Gem}} + C_{Gem}^{\gamma_{Gem}}} \tag{10b}$$

Data analysis

The pharmacodynamic model was fitted simultaneously to all data obtained for both drugs, alone and in combination, using ADAPT-5 (version 5.0.49) [25]. Modeling was performed using the maximum likelihood method. Analysis

was based on a naïve pooled approach. The variance models were defined as:

$$V_i = (\sigma \cdot Y(t_i))^2$$

where V_i is the variance at i th time point t_i , σ is the variance parameter, and Y is the model-predicted cell number. Selection criteria during model development were based on goodness-of-fit plots, changes in the objective function value, the Akaike Information Criteria (AIC), and coefficients of variation (CV %). Because of the large number of differential equations and data, appropriate changes were made to the global settings of ADAPT-5. For example, the maximum number of differential equations was 224 and the maximum number of output equations was 32. Simulations were also performed in Matlab 7.8.0 (MathWorks, Natick, MA).

Results

Determination of IC_{50} concentrations

The MiaPaCa-2 and BxPC-3 cell lines were exposed to a wide range of single-agent concentrations for 3 days before

they were harvested and counted. The concentration–effect curves are shown in Fig. 2. Parameter estimates are summarized in Table 2. The IC_{50} of gemcitabine was 22.7 nM for MiaPaCa-2 and 16.8 nM for BxPC-3 cells. The IC_{50} of trabectedin was 0.851 nM for MiaPaCa-2 and 0.599 nM for BxPC-3 cells. In both cell lines, trabectedin was more efficacious than gemcitabine; the I_{max} for trabectedin was 0.965 in MiaPaCa-2 and 0.964 in BxPC-3 cells, whereas I_{max} for gemcitabine was 0.637 in MiaPaCa-2 and 0.810 in BxPC-3 cells.

Single and combination drug effects on cell proliferation

The PD model shown in Fig. 1 was used to fit the time course of cell number change simultaneously for 8 concentrations of gemcitabine, 8 concentrations of trabectedin, and 16 combinations. The model was able to characterize well the delayed, concentration-dependent cell killing effects of gemcitabine and trabectedin both as single agents (Fig. 3) and in combination (Figs. 4, 5). In the absence of drug, cell growth to steady state occurred and was fitted with the logistic growth function (Eq. 2). The R_{ss} was 1.296×10^6 cells/mL for MiaPaCa-2 and

Fig. 2 Concentration–response curves of gemcitabine and trabectedin for MiaPaCa-2 (*upper panel*) and BxPC-3 (*lower panel*) cells after 3-day exposure to single agents. Symbols represent experimental data, and lines show fitted curves Eq. (1)

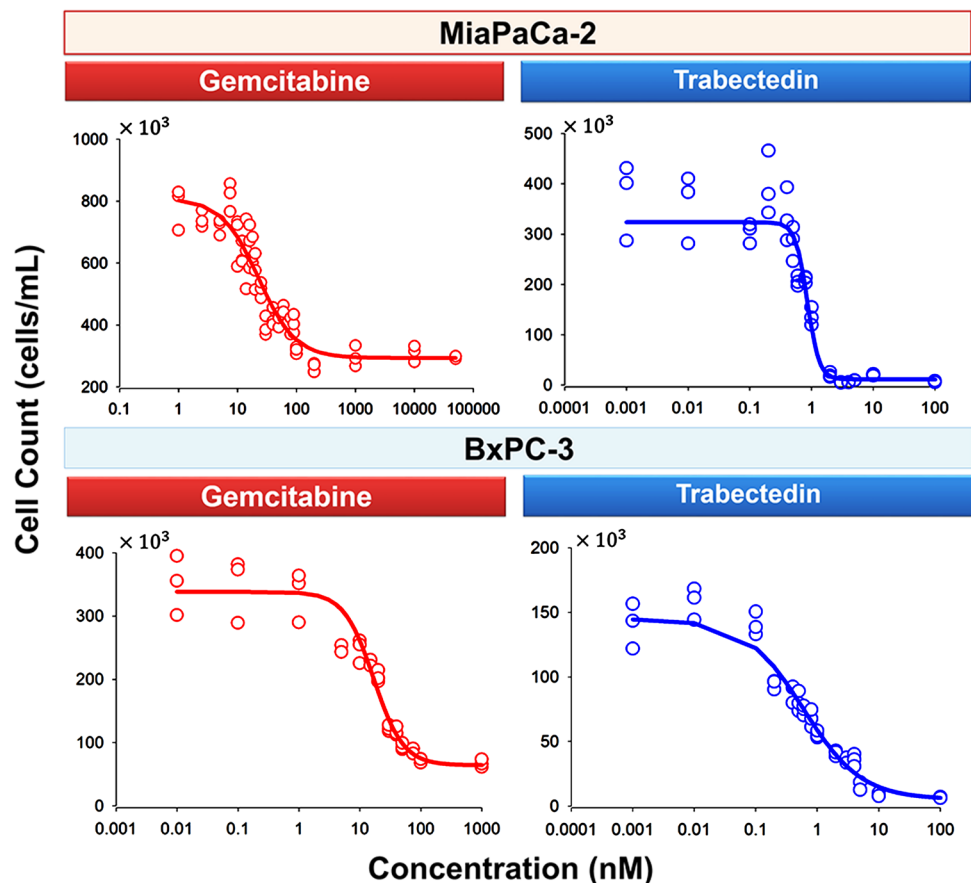
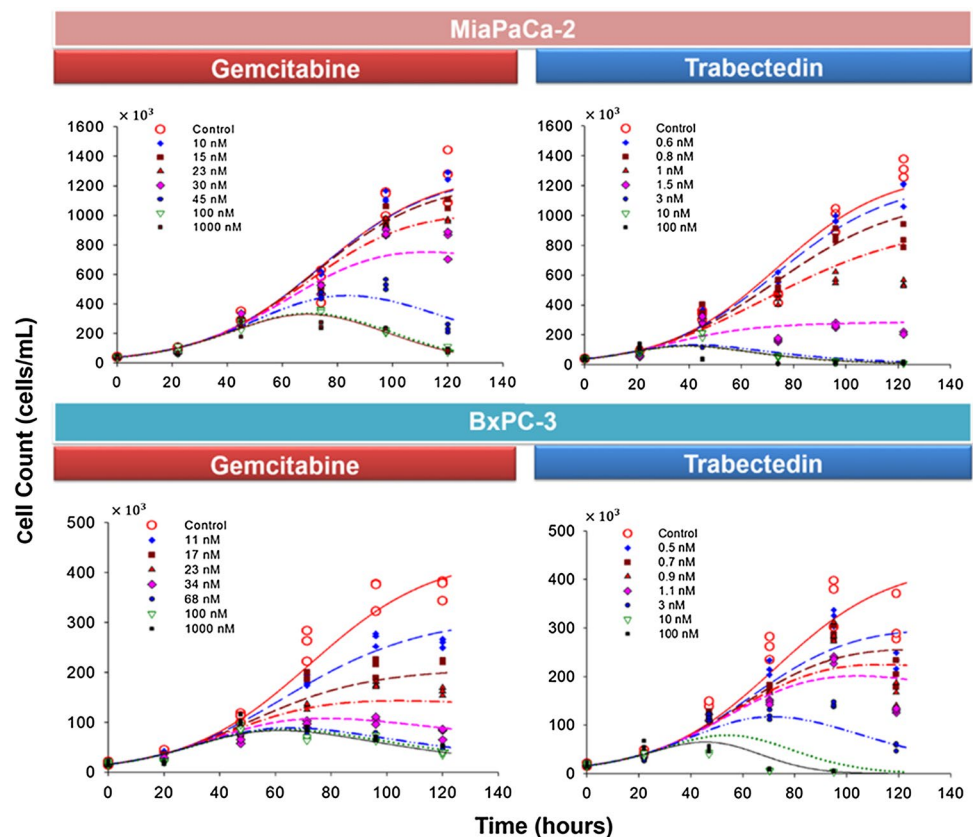


Table 2 Parameter estimates from the single-time assessments Eq. (1) for the individual drugs in two cell lines

Cell line		Estimate (CV %)	
Parameter (units)	Definition	MiaPaCa-2	BxPC-3
$R_{0,Gem}$ (cells $\times 10^{-3}/mL$)	Cell number in the absence of gemcitabine on day 3	809 (3.59)	339 (2.89)
$I_{max,Gem}$	Maximum inhibition effect of gemcitabine	0.637 (3.01)	0.810 (1.51)
$IC_{50,Gem}$ (nM)	Gemcitabine concentration at half-maximal effect	22.7 (11.9)	16.8 (7.16)
γ_{Gem}	Hill coefficient for gemcitabine	1.38 (11.0)	1.79 (9.03)
$R_{0,Et743}$ (cells $\times 10^{-3}/mL$)	Cell number in the absence of Et-743 on day 3	324 (7.46)	145 (6.10)
$I_{max,Et743}$	Maximum inhibition effect of Et-743	0.965 (0.433)	0.964 (0.731)
$IC_{50,Et743}$ (nM)	Et-743 concentration at half-maximal effect	0.851 (7.04)	0.599 (17.7)
γ_{Et743}	Hill coefficient for Et-743	4.46 (15.4)	0.921 (8.42)

Fig. 3 Effects of single-agent gemcitabine and trabectedin on MiaPaCa-2 and BxPC-3 cell proliferation as a function of time. The experiment included triplicates of eight concentrations of gemcitabine and of trabectedin. Cells were harvested and counted daily for 5 days. Symbols are experimental data, and lines show fitted curves Eqs. (2) and (3)



4.336×10^5 cells/mL for BxPC-3 cells. The doubling time of cells in the exponential growth phase, calculated using the formula $T_d = \ln(2)/k_g$, was 14.6 h for MiaPaCa-2 and 15.4 h for BxPC-3 cells.

In order to examine drug effects over a longer period of time, cells were exposed to drug for up to 5 days (Fig. 3). Cell growth data were fitted with Eq. (3) in order to identify the temporal characteristics of drug effects. The threshold concentration C_T of gemcitabine was 32.3 nM for MiaPaCa-2 and 32.9 nM for BxPC-3 cells, whereas the C_T of trabectedin was 1.70 nM for MiaPaCa-2 and 1.40 nM for

BxPC-3 cells. When $C < C_T$ for gemcitabine, i.e., when the concentration was smaller than 32.3 nM for MiaPaCa-2 and 32.9 nM for BxPC-3 cells, the drug slows the net cell growth rate in a concentration-dependent manner. Under these conditions, cells in drug-exposed groups proliferated with a slower rate than did the vehicle control group, reaching a new plateau R'_{ss} that was greater than R_0 ($R_0 = 38.4 \times 10^3$ cells/mL for MiaPaCa-2 and 16.0×10^3 cells/mL for BxPC-3). Similar results were observed for trabectedin when concentrations were smaller than the C_T of 1.70 nM for MiaPaCa-2 and 1.40 nM for

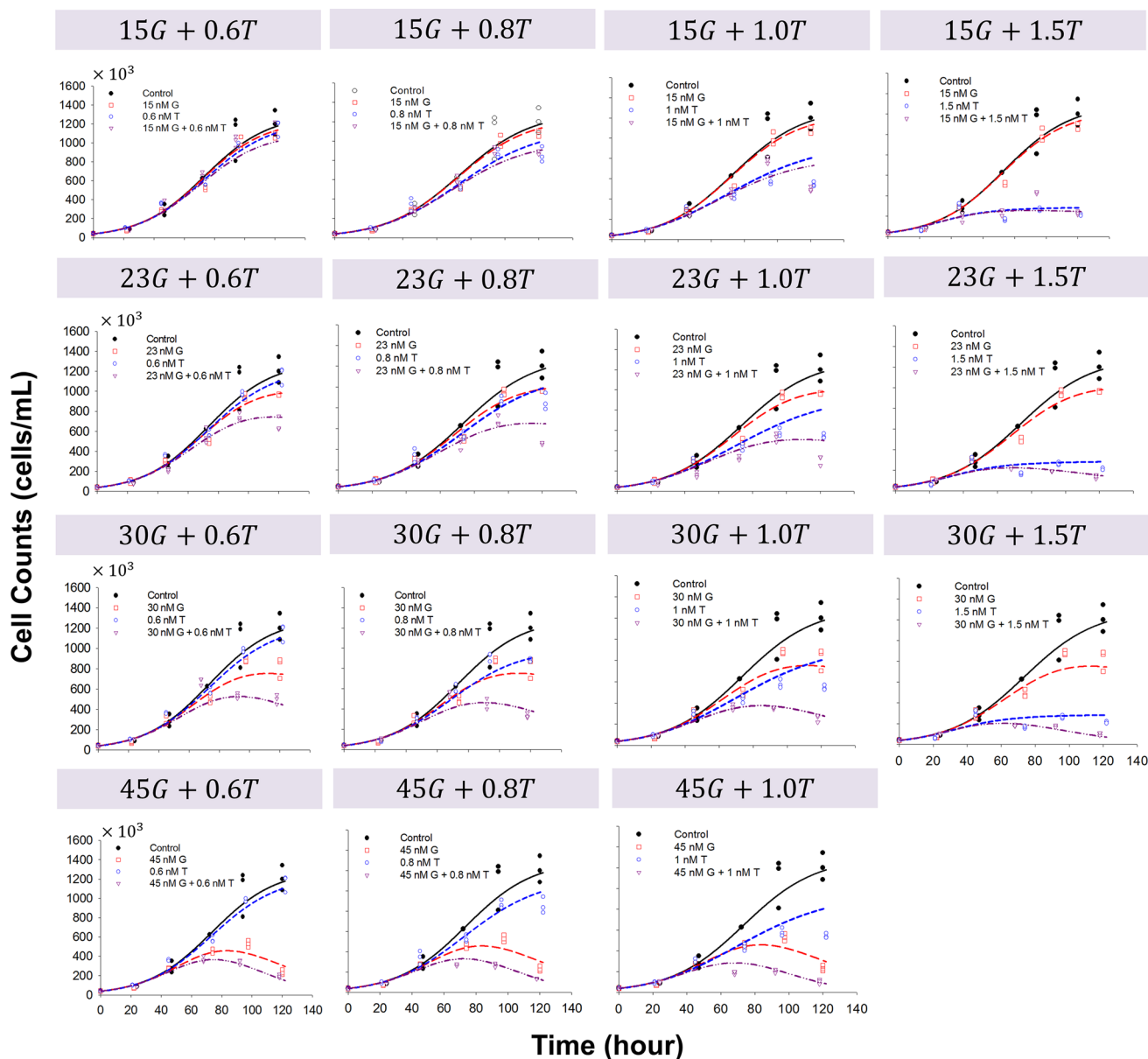


Fig. 4 Effects of gemcitabine (G) in combination with trabectedin (T) on MiaPaCa-2 cell proliferation versus time. Symbols are experimental data, and lines show fitted curves Eqs. (2) and (4)

BxPC-3 cells. Conversely, if $C > C_T$, the drugs induced mainly cytotoxic effects and the cell numbers declined toward a new steady state that was smaller than R_0 . Cells incubated with supra-threshold concentrations of gemcitabine (>32.3 nM for MiaPaCa-2 and >32.9 nM for BxPC-3) or trabectedin (>1.70 nM for MiaPaCa-2 and >1.40 nM for BxPC-3) initially exhibited increases in cell number because of the temporal delay in effect, but once the cytotoxic effects were established, cell numbers declined toward a new plateau (R'_{ss}) that was below the initial baseline.

Simultaneous fitting of all data with Eqs. (3) and (4) gave reasonable parameter estimates (Table 3) with good

precision. All CV % values were less than 16 %. The estimated $K_{max,Gem}$ was 0.166 h^{-1} for MiaPaCa-2 and 0.0613 h^{-1} for BxPC-3 cells. The estimated $K_{max,E1743}$ was 0.0858 h^{-1} for MiaPaCa-2 and 0.261 h^{-1} for BxPC-3 cells. The estimated values of the KC_{50} (Table 3) indicate different sensitivities of the two cell lines to the drugs as single agents. BxPC-3 cells were more sensitive to gemcitabine and less sensitive to trabectedin than were MiaPaCa-2 cells: $KC_{50,Gem}$ was 41.5 nM for MiaPaCa-2 and 21.4 nM for BxPC-3 cells, whereas the $KC_{50,E1743}$ was 1.63 nM for MiaPaCa-2 and 6.31 nM for BxPC-3 cells. Despite similar doubling times for the two cell lines, the temporal delay of

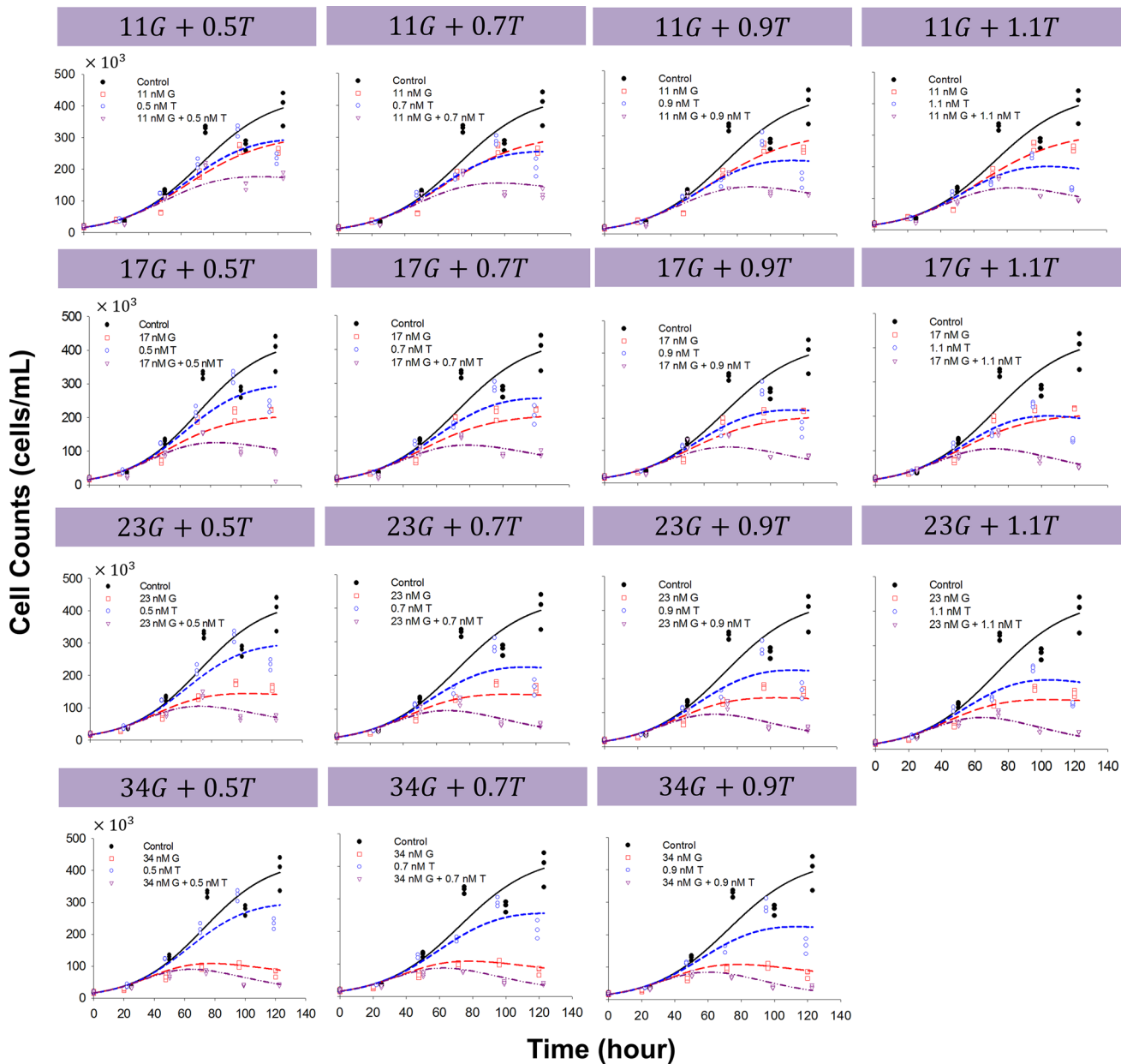


Fig. 5 Effects of gemcitabine (G) in combination with trabectedin (T) on BxPC-3 cell proliferation versus time. *Symbols* are experimental data, and *lines* show fitted curves Eqs. (2) and (4)

gemcitabine effects (4τ) was longer for MiaPaCa-2 than for BxPC-3 cells; τ was 29.2 h for MiaPaCa-2 and 14.9 h for BxPC-3 cells. For trabectedin, τ was 10.7 h for MiaPaCa-2 and 22.1 h for BxPC-3 cells.

Cells were also exposed to combinations of both agents for up to 5 days, and the data for the single and combined drugs were fitted simultaneously with the model (Fig. 1) as implemented in Eq. (4). Figure 4 shows the effect of gemcitabine combined with trabectedin on cell proliferation as a function of exposure time for MiaPaCa-2 cells, and Fig. 5 shows the data for BxPC-3 cells. The final

parameters are summarized in Table 3. The interaction parameter ψ was 0.806 (confidence interval 0.742–0.870) for MiaPaCa-2 and 0.843 (confidence interval 0.698–0.990) for BxPC-3 cells, suggesting that the combination of gemcitabine and trabectedin exerts modest synergistic effects. If ψ was set equal to 1, the model under-predicted the efficacy data compared to model predictions using the estimated ψ .

Simulations were performed to illustrate how to find combined concentrations that can mediate cytostatic effects vs. cytotoxic effects. Three-dimensional plots of

Table 3 Pharmacodynamic model parameter estimates for time-course studies Eqs. (3) and (4) for the two cell lines

Cell line		Estimate (CV %)	
Parameter (units)	Definition	MiaPaCa-2	BxPC-3
k_g (h^{-1})	Growth rate constant	0.0475 (1.44)	0.0451 (2.17)
R_0 (cells $\times 10^{-3}/mL$)	Cell number on day zero when drug was added	38.4 (1.00)	16.0 (1.62)
$K_{max,Gem}$ (h^{-1})	Maximal cell kill constant for gemcitabine	0.166 (15.6)	0.0613 (5.53)
$KC_{50,Gem}$ (nM)	Gemcitabine concentration inducing 50 % of $K_{max,Gem}$	41.5 (3.61)	21.4 (6.59)
γ_{Gem}	Hill coefficient for gemcitabine	3.82 (6.70)	2.07 (7.72)
$1/\tau_{Gem}$ (h^{-1})	Transit constant for gemcitabine	0.0343 (8.47)	0.0671 (5.92)
$K_{max,Et743}$ (h^{-1})	Maximal cell kill constant for Et-743	0.0858 (2.50)	0.261 (17.0)
$KC_{50,Et743}$ (nM)	Et-743 concentration inducing 50 % of $K_{max,Et743}$	1.63 (1.39)	6.31 (10.6)
γ_{Et743}	Hill coefficient for Et-743	3.60 (5.06)	1.07 (7.38)
$1/\tau_{Et743}$ (h^{-1})	Transit constant for Et-743	0.0932 (3.86)	0.0452 (9.44)
ψ	Interaction parameter	0.806 (3.96)	0.843 (8.64)
R_{ss} (cells $\times 10^{-3}/mL$)	Cell number at steady state	1296 (3.95)	433.6 (6.35)

the combined concentrations necessary to achieve R'_{ss} are shown in Fig. 6a for MiaPaCa-2 cells and Fig. 6b for BxPC-3 cells. Surfaces represent the model predictions using Eq. (8) based on the fitted parameters (Table 3). Figure 6c is a bird's eye view of the three-dimensional plot, in which each line represents one surface that cuts through the three-dimensional plot, and the area is composed of numerous lines. If the combined concentrations of drug A ($C_{drug A}$) and drug B ($C_{drug B}$) fall on the solid line at the middle, then the combination will cause cells to reach a steady state R'_{ss} that is equal to R_0 . If the combined concentrations fall into the green area that is below the solid line, then the combination will cause cells to reach a value of R'_{ss} that is greater than R_0 , i.e., the drugs combined cause only cytostatic effects. However, if the combined concentrations fall into the red area that is above the solid line, then the combination will cause cells to reach a value of R'_{ss} that is smaller than R_0 . In that case, the drug combination exerts cytotoxic effects.

Discussion

Traditional modeling approaches to characterize drug combinations that do not account for time-dependent effects upon cell proliferation and death are inadequate. A preferred PD model should be able to characterize time-dependent profiles [16, 23, 26, 27]. The model described here (Fig. 1) is able to account for both time and concentration dependency. The model allows simultaneous fitting of temporal cell growth data for multiple concentrations of two drugs as single agents and combined (Figs. 3, 4, 5). The estimated parameters are time-averaged and concentration-averaged values that capture the entire array of data.

Two pancreatic cancer cell lines (MiaPaCa-2 and BxPC-3) were selected for study based upon their phenotypic and genotypic differences [28]. MiaPaCa-2 has mutant Kras and p53 genes and a wild-type smad 4 gene, whereas BxPC-3 has wild-type Kras and p53 genes and a mutant smad 4 gene.

In both cell lines (Fig. 4 for MiaPaCa-2 and Fig. 5 for BxPC-3), cell numbers grew to a plateau in the absence of drug. Therefore, the drug-free control data were modeled with the logistic growth function. Time delays between the initial drug exposure and effects observed after various incubation times were modeled with transit steps. Cytotoxic effects were characterized using a nonlinear cytotoxic function [19, 27, 29] that enables characterization of cell growth and death after exposure to various concentrations of single agents. This model feature is valuable when drug effects are both time and concentration dependent. The PD model for single-agent drugs was extended to characterize drug combination effects. Additivity was defined as the summation of the killing effects of the two cytotoxic agents, and the inclusion of an interaction parameter in the combination model enabled quantification of interaction behavior that was not additive.

The IC_{50} of the single agents was time independent for the two cell lines. The estimate of IC_{50} for trabectedin (approximately 2.3 nM) was similar to peak plasma concentrations achieved after 24 h of continuous infusions in patients with solid tumors [30]. The IC_{50} values of gemcitabine for both cell lines (Table 2) are in good agreement with previous work that reported an IC_{50} of 40 nM in MiaPaCa-2 cells and 18 nM in BxPC-3 cells [31]. Thus MiaPaCa-2 cells were relatively resistant to gemcitabine compared to BxPC-3 cells.

Identifying experiment-independent, compound-specific drug action and interaction parameters can assist

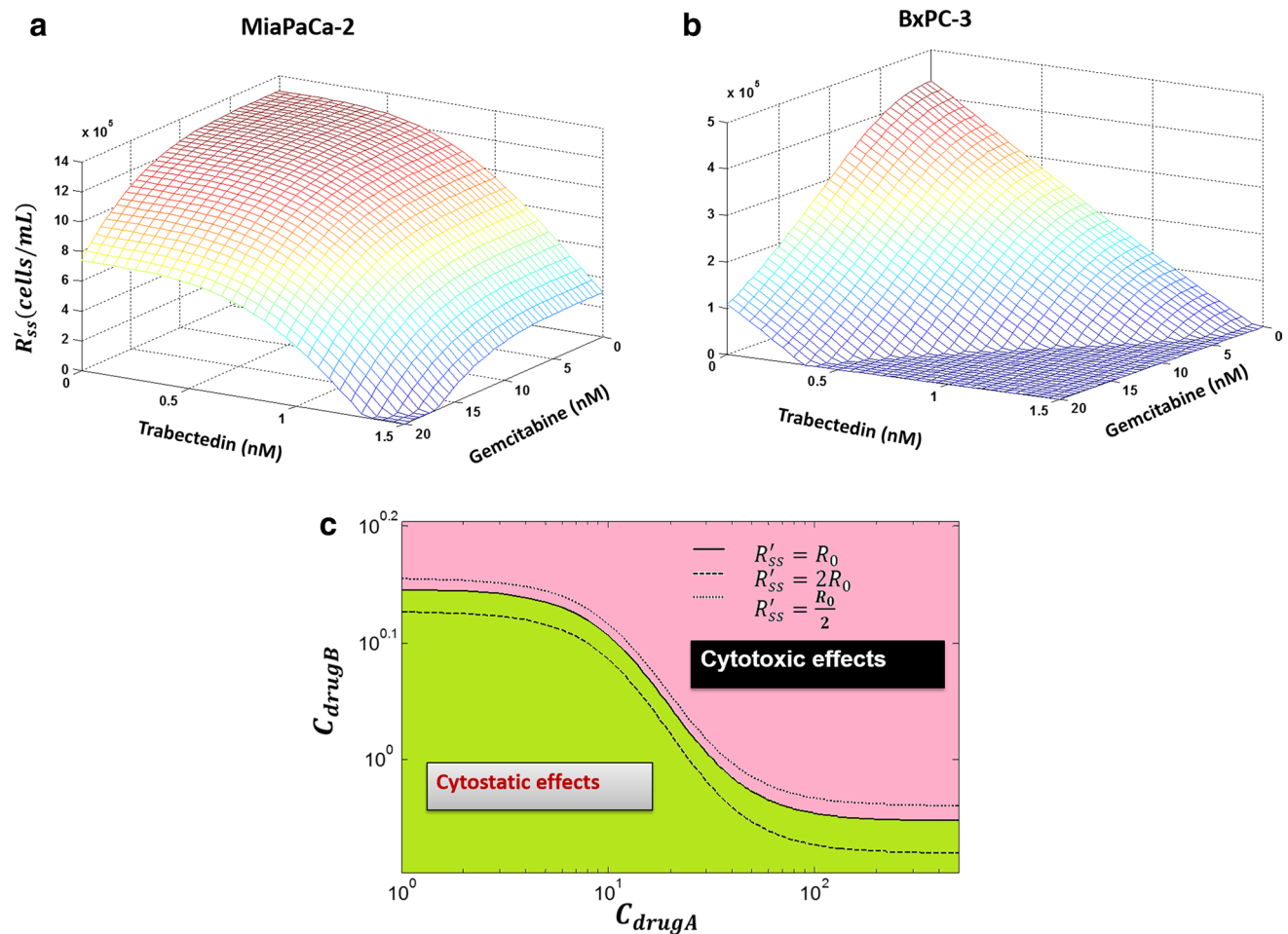


Fig. 6 Relationship between combined concentrations and R'_{ss} . **a, b** Three-dimensional plots of drug concentrations required in the combinations to achieve a new steady state R'_{ss} . Surfaces are the model simulations based on the fitted parameters (Table 3) for MiaPaCa-2 (**a**) and BxPC-3 (**b**) cells. **c** Simulation of all possible combinations of two drugs (C_{drugA} and C_{drugB}) that result in the indicated cell steady states R'_{ss} . If the combined drug A (C_{drugA}) and drug B concen-

trations (C_{drugB}) fall on the *solid line* at the middle, then the combination will cause cells to reach a steady state R'_{ss} that is equal to R_0 . If the combined concentrations fall into the *green area* that is below the *solid line*, the combination only causes cytostatic effects. Otherwise, if the combined concentrations fall into the *red area* that is above the *solid line*, the combination exerts cytotoxic effects

preclinical to clinical translation [32]. Conversely, inappropriate experimental conditions that provide erroneous potency-related parameters may confound correlation of preclinical and clinical results. Conventional drug–drug interaction models such as Loewe additivity [14] and isobolograms [15] yield parameters such as IC_{50} that are useful for the purpose of compound screening [33]. However, parameters such as IC_{50} can be experiment-dependent as they may vary with exposure times. In the present work, we obtained IC_{50} values for two cell lines (Table 2) from time-independent data and simple equation fitting (Eq. 1), as well as KC_{50} values (Table 3) from time-dependent data and dynamic modeling (Eqs. 3–4). The IC_{50} values served as a guide to select concentrations that would span the concentration–response range (Fig. 2) and provided a basis for devising a maximally informative array of combination

pairs (Table 1) for time-dependent studies (Figs. 3, 4, 5). Additionally, the dynamic combination model was fitted to pooled cell count data, as opposed to frequently employed approaches in which the PD endpoints consist of cell counts for treated groups that are normalized by averaged responses of control groups. Such normalization imposes the variability of the control group on all groups that are normalized. This additional source of variability is avoided by fitting the cell count data itself [34]. A wide range of concentrations (Table 1) was examined to detect saturation of the cytotoxic effects. The proposed PD model described the observed data well (Figs. 3, 4, 5) and provided reasonable parameter estimates with good precision (Table 3). The estimated KC_{50} of trabectedin was smaller than that of gemcitabine: it was 25.5-fold lower for MiaPaCa-2 cells and 3.4-fold lower for BxPC-3 cells. This indicates not

only that trabectedin is more potent than gemcitabine, but also that its potency relative to a second drug can vary with cell line. Comparing the estimated KC_{50} for the same drug between two different cell lines showed the KC_{50} of gemcitabine for BxPC-3 to be significantly smaller than that for MiaPaCa-2 cells (Table 3), verifying that BxPC-3 cells (wild-type Kras) are more sensitive to gemcitabine than MiaPaCa-2 (mutant Kras). Conversely, the estimated KC_{50} of trabectedin in BxPC-3 is significantly larger than that for MiaPaCa-2 cells, indicating that BxPC-3 are more resistant to trabectedin than are MiaPaCa-2 cells.

Selection of drug candidates that interact synergistically with gemcitabine poses challenges. Previous publications indicate that promising combination candidates may be agents that are S-phase cell cycle specific [35] or are drugs that are able to overcome gemcitabine resistance [36]. Trabectedin is an exceedingly potent DNA-binding anticancer drug that is effective in the nanomolar range, and exerts cytotoxic effects upon many drug-resistant cancer cell lines. The hypothesis that led to our investigation of gemcitabine combined with trabectedin is based upon the molecular mechanism of trabectedin, which involves NF- κ B inhibition, caspase 3/7 activation [12], and cell cycle checkpoint activation [11]. Both gemcitabine and trabectedin target DNA and lead to double-stranded DNA breaks. In addition, up-regulation of NF- κ B and Akt/PI3K often occurs after gemcitabine treatment [37–39]. A previous study showed that trabectedin inhibited NF- κ B signaling via inhibition of I κ B α phosphorylation and induction of caspase 3/7 activation in cervical cancer cells [12]. Both NF- κ B and Akt/PI3K play a critical role in gemcitabine resistance [38, 39], and inhibition of NF- κ B by trabectedin may enhance sensitivity to gemcitabine. In addition, gemcitabine and trabectedin may exert a synergistic effect upon the activation of the caspase 3 pathway. Finally, gemcitabine is a cell cycle-specific agent; it activates cell cycle checkpoints through the activation of the ATM/CHK2–ATR/CHK1 pathway [40]. Trabectedin induces cell cycle arrest at S and G2/M phases, which may help to synchronize cancer cells in S-phase so that gemcitabine incorporation into DNA may increase. Future studies will investigate drug combination effects on the cell cycle distribution and specific signaling pathways.

Several caveats apply to our PD study and analysis. First, cytoplasmic effect-site gemcitabine concentrations were assumed to equal the extracellular concentrations in media, and were assumed to be constant over the duration of the experiment. However, it is the gemcitabine triphosphate metabolite dFdCTP that is incorporated into DNA and causes the PD effects. Thus an improvement could be to obtain intracellular concentrations of dFdCTP, as was done by Battaglia et al. [41], and utilize dFdCTP incorporation

into DNA to drive the PD effects in the model. In addition, the transit compartments employed here approximate drug transport and metabolic steps that could be defined in greater detail.

Few existing PD models are able to characterize temporal pharmacodynamic effects of chemotherapeutic drug combinations in terms of cancer cell or tumor growth. The model proposed here is simple enough to enable characterization and prediction of combined drug effects, as well as assessment of the nature of the drug interaction. With regard to model generality and validity, the proposed model was able to characterize simultaneously the cell growth inhibition from 32 concentrations of two drugs, as single agents or combined, on two different pancreatic cancer cell lines. In preliminary work, the PD model has also been applied to the combination of gemcitabine with two other agents, and successfully characterized and predicted drug interactions (*unpublished*). It provides a means to select quickly those potential agents within a pool of candidates that may possess the best activity in combination with another chemotherapeutic agent. The model demonstrated that gemcitabine and trabectedin interact synergistically, and the combination demonstrates enhanced anticancer activity. The concomitant administration of gemcitabine with trabectedin may thus have a potential therapeutic benefit. Finally, the use of ψ as a drug interaction measure has an additional significance. In a mechanistic PD model, values of ψ differing from unity suggest an incomplete understanding of the mechanism of action of the two compounds as implemented in the model. Thus ψ provides an indication that more detailed studies of mechanisms of action on cell cycle progression, signal transduction pathways, and other pharmacological responses require investigation and integration into the model.

Acknowledgments The authors would like to thank Prof. Wojciech Krzyzanski for valuable discussions. Trabectedin was a gift from PharmaMar. This work was supported by NIH Grants GM57980 and GM24211 to W.J.J. and CA168454 and CA198096 to R.M.S, the National Research Fund, Luxembourg, and co-funded under the Marie Curie Actions of the European Commission (FP7-COFUND).

Compliance with ethical standards

Conflict of interest No conflicts of interest are reported.

Appendix

The following provides a proof of Eqs. (5)–(10), assuming that drug concentrations are constant during experiments. The stationary equations of the proposed PD model Eqs. (3) and (4) are as below:

$$K_d = \frac{K_{\max,d} C_d^{\gamma_d}}{K C_{50,d}^{\gamma_d} + C_d^{\gamma_d}} \quad (11a)$$

$$0 = \frac{1}{\tau_d} (K_d - K_{1,d_{ss}}) \tag{11b}$$

$$0 = \frac{1}{\tau_d} (K_{1,d_{ss}} - K_{2,d_{ss}}) \tag{11c}$$

$$0 = \frac{1}{\tau_d} (K_{2,d_{ss}} - K_{3,d_{ss}}) \tag{11d}$$

$$0 = \frac{1}{\tau_d} (K_{3,d_{ss}} - K_{4,d_{ss}}) \tag{11e}$$

$$0 = k_g R'_{ss} \left(1 - \frac{R'_{ss}}{R_{ss}} \right) - \mu_{ss} R'_{ss} \tag{11f}$$

with

$$\mu_{ss} = \begin{cases} K_{4,d_{ss}} & \text{for single agent} \\ K_{4,Gem_{ss}} + K_{4,Et743_{ss}} & \text{for combination} \end{cases}$$

From Eqs. (11a)–(11e) we have

$$K_d = K_{1,d_{ss}} = \dots = K_{4,d_{ss}}$$

so that

$$\mu_{ss} = \begin{cases} \frac{K_{\max,d} C_d^{\gamma_d}}{K C_{50,d}^{\gamma_d} + C_d^{\gamma_d}} & \text{for single agent} \\ \frac{K_{\max,Gem} C_{Gem}^{\gamma_{Gem}}}{(\psi K C_{50,Gem})^{\gamma_{Gem}} + C_{Gem}^{\gamma_{Gem}}} + \frac{K_{\max,Et743} C_{Et743}^{\gamma_{Et743}}}{K C_{50,Et743}^{\gamma_{Et743}} + C_{Et743}^{\gamma_{Et743}}} & \text{for combination} \end{cases} \tag{12}$$

To calculate the new steady state for single-agents, we solve Eqs. (11f) and (12) with respect to R'_{ss} and obtain Eq. (6). In order to achieve that the number of cells decreases for $t > 0$, one needs $R'_{ss} \leq R_0$, i.e., the threshold concentration is defined via

$$R'_{ss} = \left(k_g - \frac{K_{\max,d} C_d^{\gamma_d}}{K C_{50,d}^{\gamma_d} + C_d^{\gamma_d}} \right) \frac{R_{ss}}{k_g} = R_0$$

which is equivalent to

$$k_g (R_{ss} - R_0) K C_{50,d}^{\gamma_d} + k_g (R_{ss} - R_0) C_d^{\gamma_d} = K_{\max,d} C_d^{\gamma_d} R_{ss}.$$

This leads to

$$C_{T,d}^{\gamma_d} = \frac{k_g (R_{ss} - R_0) K C_{50,d}^{\gamma_d}}{K_{\max,d} R_{ss} - k_g (R_{ss} - R_0)}$$

as Eq. (5) is shown. To obtain total cell eradication, the concentration

$$\frac{K_{\max,d} C_d^{\gamma_d}}{K C_{50,d}^{\gamma_d} + C_d^{\gamma_d}} \geq k_g$$

is needed, i.e., $C_{E,d}$ is defined via

$$\frac{K_{\max,d} C_{E,d}^{\gamma_d}}{K C_{50,d}^{\gamma_d} + C_{E,d}^{\gamma_d}} = k_g$$

resulting in Eq. (7).

For combination effects, Eqs. (11f) and (12) provide

$$\frac{K_{\max,Gem} C_{Gem}^{\gamma_{Gem}}}{(\psi K C_{50,Gem})^{\gamma_{Gem}} + C_{Gem}^{\gamma_{Gem}}} + \frac{K_{\max,Et743} C_{Et743}^{\gamma_{Et743}}}{K C_{50,Et743}^{\gamma_{Et743}} + C_{Et743}^{\gamma_{Et743}}} = k_g \left(1 - \frac{R'_{ss}}{R_{ss}} \right). \tag{13}$$

and Eq. (9) is obtained.

References

1. Siegel R, Ma J, Zou Z, Jemal A (2014) Cancer statistics, 2014. *CA Cancer J Clin* 64:9–29. doi:10.3322/caac.21208 (Epub 2014 Jan 7)
2. Burris HA, Moore MJ, Andersen J, Green MR, Rothenberg ML, Modiano MR, Cripps MC, Portenoy RK, Storniolo AM, Tarassoff P, Nelson R, Dorr FA, Stephens CD, Von Hoff DD (1997) Improvements in survival and clinical benefit with gemcitabine as first-line therapy for patients with advanced pancreas cancer: a randomized trial. *J Clin Oncol* 15:2403–2413
3. Peter GJ, van der Wilt CL, van Moorsel CJ, Kroep JR, Bergman AM, Ackland SP (2000) Basis for effective combination cancer chemotherapy with antimetabolites. *Pharmacol Ther* 87:227–253
4. Rinehart KL, Holt TG, Fregeau NL, Keifer PA, Wilson GR, Perun TJ Jr, Sakai R, Thompson AG, Stroh JG, Shield LS, Seigler DS, Li LH, Martin DG, Grimmlikhuijzen CJP, Gade G (1990) Bioactive compounds from aquatic and terrestrial sources. *J Nat Prod* 53:771–792
5. Cuevas C, Francesch A (2009) Development of Yondelis (trabectedin, ET-743): a semisynthetic process solves the supply problem. *Nat Prod Rep* 26:322–337
6. Mini E, Nobili S, Caciaqli B, Landini I, Mazzei T (2006) Cellular pharmacology of gemcitabine. *Ann Oncol* 17(Suppl 5):v7–12
7. D’Incalci M, Galmarini CM (2010) A review of trabectedin (ET-743): a unique mechanism of action. *Mol Cancer Ther* 9:2157–2163
8. Yip-Schneider MT, Sweeney CJ, Jung SH, Crowell PL, Marshall MS (2001) Cell cycle effects of nonsteroidal anti-inflammatory drugs and enhanced growth inhibition in combination with gemcitabine in pancreatic carcinoma cells. *J Pharmacol Exp Ther* 298:976–985
9. Cappella P, Tomasoni D, Faretta M, Lupi M, Montalenti F, Viale F, Banzato F, D’Incalci M, Ubezio P (2001) Cell cycle effects of gemcitabine. *Int J Cancer* 93:401–408
10. Tavecchio M, Natoli C, Ubezio P, Erba E, D’Incalci M (2007) Dynamics of cell cycle phase perturbations by trabectedin (ET-743) in nucleotide excision repair (NER)-deficient and NER-proficient cells, unraveled by a novel mathematical simulation approach. *Cell Prolif* 40:885–904
11. Gajate C, An F, Mollinedo F (2002) Differential cytostatic and apoptotic effects of ecteinascidin-743 in cancer cells. Transcription-dependent cell cycle arrest and transcription-independent JNK and mitochondrial mediated apoptosis. *J Biol Chem* 277:41580–41589
12. Miller SC, Huang R, Sakamuru S, Shukla SJ, Attene-Ramos MS, Shinn P, Van Leer D, Leister W, Austin CP, Xia M (2010)

- Identification of known drugs that act as inhibitors of NF-kappaB signaling and their mechanism of action. *Biochem Pharmacol* 79:1272–1280
13. Messersmith WA, Jimeno A, Ettinger D, Laheru D, Brahmer J, Lansley D, Khan Y, Donehower RC, Elsayed Y, Zannikos P, Hidalgo M (2008) Phase I trial of weekly trabectedin (E7-743) and gemcitabine in patients with advanced solid tumors. *Cancer Chemother Pharmacol* 63:181–188
 14. Loewe S (1953) The problem of synergism and antagonism of combined drugs. *Arzneimittelforschung* 3:285–290
 15. Gessner PK (1974) The isobolographic method applied to drug interactions. In: Moselli PL, Garattini S, Cohen SN (eds) *Drug interactions*. Raven Press, New York, pp 349–362
 16. Terranova N, Germani M, Del Bene F, Magni P (2013) A predictive pharmacokinetic-pharmacodynamic model of tumor growth kinetics in xenograft mice after administration of anticancer agents given in combination. *Cancer Chemother Pharmacol* 72:471–482
 17. Earp J, Krzyzanski W, Chakraborty A, Zamacona MK, Jusko WJ (2004) Assessment of drug interactions relevant to pharmacodynamics indirect response models. *J Pharmacokinet Pharmacodyn* 31:345–380
 18. Goteti K, Garner CE, Utley L, Dai J, Ashwell S, Moustakas DT, Gönen M, Schwartz GK, Kern SE, Zabludoff S, Brassil PJ (2010) Preclinical pharmacokinetic/pharmacodynamic models to predict synergistic effects of co-administered anti-cancer agents. *Cancer Chemother Pharmacol* 66:245–254. doi:10.1007/s00280-009-1153-z
 19. Lobo ED, Balthasar JP (2002) Pharmacodynamic modeling of chemotherapeutic effects: application of a transit compartment model to characterize methotrexate effects in vitro. *AAPS PharmSci* 4:E42
 20. Koch G, Walz A, Lahu G, Schropp J (2009) Modeling of tumor growth and anticancer effects of combination therapy. *J Pharmacokinet Pharmacodyn* 36:179–197
 21. Chakraborty A, Jusko WJ (2002) Pharmacodynamic interaction of recombinant human interleukin-10 and prednisolone using in vitro whole blood lymphocyte proliferation. *J Pharm Sci* 91:1334–1342
 22. Robertson TB (1923) *The chemical basis of growth and senescence*. J B Lippincott Company, Philadelphia
 23. Simeoni M, Magni P, Cammia C, De Nicolao G, Croci V, Presenti E, Germani M, Poggesi I, Rocchetti M (2004) Predictive pharmacokinetic-pharmacodynamic modeling of tumor growth kinetics in xenograft models after administration of anticancer agents. *Cancer Res* 64:1094–1101
 24. Rocchetti M, Simeoni M, Pesenti E, De Nicolao G, Poggesi I (2007) Predicting the active doses in humans from animal studies: a novel approach in oncology. *Eur J Cancer* 43:1862–1868
 25. D'Argenio DZ, Schumitzky A, Wang X (2009) ADAPT 5 user's guide: pharmacokinetic/pharmacodynamics systems analysis software. Biomedical Simulations Resource, Los Angeles
 26. Ait-Oudhia S, Straubinger RM, Mager DE (2013) Systems pharmacological analysis of paclitaxel-mediated tumor priming that enhances nanocarrier deposition and efficacy. *J Pharmacol Exp Ther* 344:103–112. doi:10.1124/jpet.112.199109 (Epub 2012 Oct 3)
 27. Jusko WJ (1971) Pharmacodynamics of chemotherapeutic effects: dose-time–response relationships for phase-nonspecific agents. *J Pharm Sci* 60:892–895
 28. Deer EL, González-Hernández J, Coursen JD, Shea JE, Ngatia J, Scaife CL, Firpo MA, Mulvihill SJ (2010) Phenotype and genotype of pancreatic cancer cell lines. *Pancreas* 39:425–435. doi:10.1097/MPA.0b013e3181c15963
 29. Zhi JG, Nightingale CH, Quintilani R (1988) Microbial pharmacodynamics of piperacillin in neutropenic mice of systematic infection due to *Pseudomonas aeruginosa*. *J Pharmacokinet Biopharm* 16:355–375
 30. Taamma A, Misset JL, Riofrio M, Guzman C, Brain E, Lopez Lazaro L, Rosing H, Jimeno JM, Cvitkovic E (2001) Phase I and pharmacokinetic study of ecteinascidin-743, a new marine compound, administered as a 24-hour continuous infusion in patients with solid tumors. *J Clin Oncol* 19:1256–1265
 31. Duxbury MS, Ito H, Zinner MJ, Ashley SW, Whang EE (2004) Inhibition of SRC tyrosine kinase impairs inherent and acquired gemcitabine resistance in human pancreatic adenocarcinoma cell. *Clin Cancer Res* 10:2307–2318
 32. Simeoni M, De Nicolao G, Magni P, Rocchetti M, Poggesi I (2013) Modeling of human tumor xenografts and dose rationale in oncology. *Drug Discov Today Technol* 10:e365–e372. doi:10.1016/j.dtt.2012.07.004
 33. Del Bene F, Germani M, De Nicolao G, Magni P, Re CE, Ballinari D, Rocchetti M (2009) A model-based approach to the in vitro evaluation of anticancer activity. *Cancer Chemother Pharmacol* 63:827–836
 34. Woo S, Pawaskar D, Jusko WJ (2009) Methods of utilizing baseline values for indirect response models. *J Pharmacokinet Pharmacodyn* 36:381–408
 35. Huang P, Plunkett W (1995) Induction of apoptosis by gemcitabine. *Semin Oncol* 22(4 Suppl 11):19–25
 36. Bergman AM, Pinedo HM, Peters GJ (2002) Determinants of resistance to 2',2'-difluorodeoxycytidine (gemcitabine). *Drug Resist Updates* 5:19–33
 37. Arlt A, Gehrz A, Muerkoster S, Vorndamm J, Kruse ML, Fölsch UR, Schäfer H (2003) Role of NF-kappaB and Akt/P13K in the resistance of pancreatic carcinoma cell lines against gemcitabine-induced cell death. *Oncogene* 22:3243–3251
 38. Chen D, Niu M, Jiao X, Zhang K, Liang J, Zhang D (2012) Inhibition of AKT2 enhances sensitivity to gemcitabine via regulating PUMA and NF-kB signaling pathway in human pancreatic ductal adenocarcinoma. *Int J Mol Sci* 13:1186–1208. doi:10.3390/ijms13011186 (Epub 2012 Jan 20)
 39. Kagawa S, Takano S, Yoshitomi H, Kimura F, Satoh M, Shimizu H, Yoshidome H, Ohtsuka M, Kato A, Furukawa K, Matsushita K, Nomura F, Miyazaki M (2012) Akt/mTOR signaling pathway is crucial for gemcitabine resistance induced by Annexin II in pancreatic cancer cells. *J Surg Res* 178:758–767. doi:10.1016/j.jss.2012.05.065 (Epub 2012 Jun 12)
 40. Karnitz LM, Flatten KS, Wagner JM, Loegering D, Hackbarth JS, Arlander SJ, Vroman BT, Thomas MB, Baek YU, Hopkins KM, Lieberman HB, Chen J, Cliby WA, Kaufmann SH (2005) Gemcitabine-induced activation of checkpoint signaling pathways that affect tumor cell survival. *Mol Pharmacol* 68:1636–1644
 41. Battaglia MA, Parker RS (2011) Pharmacokinetic/pharmacodynamic modelling of intracellular gemcitabine triphosphate accumulation: translating in vitro to in vivo. *IET Syst Biol* 5:34. doi:10.1049/iet-syb.2009.0073